STEM CELLS AND DEVELOPMENT
Volume 21, Number 11, 2012
© Mary Ann Liebert, Inc.
DOI: 10.1089/scd.2011.0505

Laminin-111 Stimulates Proliferation of Mouse Embryonic Stem Cells Through a Reduction of Gap Junctional Intercellular Communication via RhoA-Mediated Cx43 Phosphorylation and Dissociation of Cx43/ZO-1/Drebrin Complex

Han Na Suh,[1] Mi Ok Kim,[1] and Ho Jae Han[2]

Abstract

Gap junctions within extracellular matrix (ECM)-defined boundaries ensure synchronous activity between cells destined to become functional mediators that regulate cell behavior. However, the role of ECM in connexin (Cx) function in mouse embryonic stem cells (mESCs) has not been elucidated. Therefore, we examined the role of laminin-111 in the control of Cx43 functions and related signal pathways in mESCs. ECM components (laminin-111, fibronectin, and collagen I) increased Cx43 phosphorylation and decreased Lucifer yellow (Ly) diffusion. In addition, laminin-111 increased the proliferation index through reduction of gap junctional intercellular communication (GJIC), which was confirmed by 18α-glycyrrhetinic acid (18α-GA). Laminin-111 increased phosphorylation of focal adhesion kinase (FAK)/Src and protein kinase C (PKC), which were inhibited by integrin β1 antibody (Ab) and laminin receptor-1 (LR-1) Ab, respectively. In addition, inhibition of both FAK/Src and PKC blocked Cx43 phosphorylation. Laminin-111 increased the Ras homolog gene family, member A (RhoA) activation, which was blocked by FAK/Src and PKC inhibitors, suggesting the existence of parallel pathways that merge at RhoA. Inhibition of RhoA reversed the laminin-111-induced increase of Cx43 phosphorylation and reduction of GJIC. Laminin-111 also stimulated the dissociation of Cx43/ZO-1 complex followed by disruption of Cx43/drebrin and Cx43/F-actin complexes, which were reversed by C3 (RhoA inhibitor). ZO-1 small interfering (si) RNA significantly decreased Ly diffusion. Moreover, laminin-111 decreased Cx43 labeling at the intercellular junction, whereas pretreatment with degradation inhibitors (lysosomal protease inhibitor, chloroquine; proteasome inhibitor, lactacystin) increased Cx43 expression, reversely. In conclusion, laminin-111 stimulated mESC proliferation through a reduction of GJIC via RhoA-mediated Cx43 phosphorylation and Cx43/ZO-1/drebrin complex instability-mediated Cx43 degradation.

Introduction

Cells in their normal physiological context within a tissue receive micro-environmental cues from soluble mediators, extracellular matrix (ECM), and neighboring cells. ECM had generally been thought of as solely providing a physical framework; however, now ECM is thought to be capable of exerting functional change, a process called matricrine signaling, via several mechanisms [1–2]. ECM serves as a storage depot for transient components such as growth factors, cytokines, chemokines, and enzymes. Resident proteins bind to some of these molecules and modulate their activity, bioavailability, or presentation to cell surface receptors. The active interplay between cells and the ECM culminates in intracellular events associated with signal transduction cascades, which, in turn, regulate the expression of genes necessary for cell differentiation, proliferation, and survival [3]. A major problem concerning the use of ECM proteins for technological purposes is the lack of availability of pure native isoforms for such purposes, which can yield variable and irreproducible results. Laminins are a large family of heterotrimeric macromolecules that have 15

[1]Department of Veterinary Physiology, College of Veterinary Medicine, Chonnam National University, Gwangju, South Korea.
[2]Department of Veterinary Physiology, College of Veterinary Medicine and Research Institute for Veterinary Science, Seoul National University, Seoul, South Korea.

isoforms composed of α, β, and γ chains. Different laminins show various spatiotemporal expression patterns as well as tissue-specific locations and functions. At present, mouse EHS sarcoma-derived laminin-111 is the only laminin isoform commercially available in pure native form for cell culture use, although only recently, human/mouse hybrid laminin-111 (early embryo) [4], human laminin-211 (basement membrane of muscle cells and motor-neuron synapses) [5], laminin-332 (subepithelial basement membranes) [6], laminin-411 (subendothelial basement membranes) [7], and the ubiquitous laminin-511 [8] have been successfully produced as recombinant proteins. Thus, since our research aim is not characterization of laminin subtypes functions but the role of laminin in the control of connexin 43 (Cx43) function, we used laminin-111, which may be helpful in producing more reproducible results although laminin isoforms are tissue specific and functionally distinct.

Juxtacrine signaling mechanisms, specifically cell-ECM interactions and gap junctional intercellular communications (GJIC), act in concert to influence the developmental specification of stem cells or progenitor cells [9]. It has previously been demonstrated, in other cell types (keratinocytes, alveolar epithelial cells, and ciliated tracheal epithelial cells), that Cx expression and intercellular communication are strongly influenced by laminin-integrin interactions [10–12]. This is an important issue, because embryonic stem cells (ESCs) are routinely expanded in the absence of exogenous ECM, while functional assessment of cell-cell signaling pathways often involves re-plating on adhesive substrates. Gap junctions (GJs) are specialized domains in the plasma membrane containing intercellular channels between neighboring cells in almost every tissue of multicellular organisms that allow the passage of small molecules (up to ~1 kDa), including second messengers, nucleotides, and ions [13]. GJs are thought to be important in embryonic development, cellular growth control, and differentiation [14–16]. Modulation of channel properties by protein phosphorylation/dephosphorylation, as has been shown for several Cx-formed channels [17–18], requires complexing of proteins, where Cxs are localized proximal to auxiliary proteins, such as enzymes or scaffolding proteins. Serine/threonine kinases such as protein kinase C (PKC), c-Src, and mitogen-activated protein kinase phosphorylate Cx43 and modulate GJs in sequence. In addition, many Cx43-interacting proteins, including ZO-1, drebrin, and cadherin associated with F-actin, are able to modulate GJs through actin cytoskeleton; thus, an understanding of the molecular mechanisms underlying their precise function is needed. However, the strict molecular interactions that occur between Cx43 and these regulatory partners are not yet well characterized. Therefore, further studies will be needed to fully understand and elaborate the molecular mechanisms involved in cross-talk between Cx43 and actin via ZO-1, which regulates plaque dynamics and assembly.

ESCs are pluripotent cells derived from inner cell masses of blastocysts or blastomeres of early mammalian embryos. These unique cells are characterized by extended undifferentiated proliferation in tissue culture and a prolonged potential to differentiate into derivatives of all three germ layers [19–20]. These characteristics make mouse embryonic stem cells (mESCs) a versatile biological system, and their use has led to major advances in cell and developmental biology. Many adult stem cells reportedly lack Cxs [21]. On the other hand, previous studies by our laboratory and others demonstrated the presence of GJIC in hESC [22–23] as well as mESC [24–26]. The most widely expressed member of the Cx family in mESCs, Cx43, has been reported to express both mRNA and protein [24]. Therefore, this study aimed at assessing the importance of laminin-111-mediated actions on proliferation of mESCs mediated by Cx43 macromolecule transition.

Materials and Methods

Materials

The mESCs (ES-E14TG2a) were obtained from the American Type Culture Collection. Fetal bovine serum (FBS) was purchased from Gibco. Laminin-111 (from Engelbreth-Holm-Swarm murine sarcoma basement membrane), laminin-511, fibronectin (from bovine plasma), collagen type I (from rat tail), protease inhibitor cocktail, 18α-glycyrrhetinic acid (18α-GA), chloroquine, and fluorescein isothiocynate (FITC)-anti-rabbit antibody (Ab) were purchased from Sigma-Aldrich. Alexa Fluor 488-anti-mouse and propidium iodide (PI) were obtained from Invitrogen. Protein phosphatase 2 (PP2), bisindolylmaleimide I, and Y27632 were obtained from Calbiochem. C3 and calpeptin were obtained from Cytoskeleton. Leukemia inhibitory factor (LIF), primary Abs against p-Cx43, Cx43, integrin β1, p-FAK, FAK, p-Src, Src, laminin receptor-1 (LR-1), PKCγ, PKCδ, PKCζ, p-PKC, PKC, RhoA, ZO-1, ZO-2, claudin, occludin, E-cadherin, β-catenin, drebrin, IgG, β-actin, and secondary Abs against horseradish peroxidase (HRP)-conjugated goat anti-rabbit Ab, goat anti-mouse IgG Ab, and lactacystin were purchased from Santa Cruz Biotechnology. F-actin was obtained from Abcam. All other reagents were of the highest purity commercially available.

mESC culture

Cells were maintained in Dulbecco's modified Eagle's medium (DMEM; Gibco-BRL) supplemented with 3.7 g/L of sodium bicarbonate, 1% penicillin/streptomycin, 1.7 mM L-glutamine, 0.1 mM β-mercaptoethanol, 5 ng/mL mouse LIF, and 15% FBS. Cells were cultured without a feeder layer for 5 days on culture dishes in an incubator maintained at 37°C with 5% CO_2. The medium was changed to serum-free standard medium (5% serum replacement instead of 15% FBS) for 24 h before an experiment.

Scrape loading/dye transfer assay

The GJIC level was measured using a slight modification of the Scrape loading/dye transfer (SL/DT) method [27–28]. Cells on 35-mm dishes were rinsed twice with 2 mL of phosphate buffered saline (PBS), and 0.05% Lucifer yellow (Ly) was then applied to the center of the dish. Scrapes were performed ensuring that a large group of confluent cells were traversed. Cells were incubated in the dye mix for precisely 1 min, rinsed quickly thrice with PBS, and finally examined by optical microscopy (FluoView 300, Olympus).

Fluorescence-activated cell sorting analysis

Cells were dissociated in 0.05% trypsin/ethylenediaminetetraacetic acid (EDTA), pelleted by centrifugation, and

resuspended at approximately 10^6 cells/mL in PBS containing 0.1% bovine serum albumin (BSA). The cells were then fixed with 70% ice-cold ethanol for 30 min at 4°C, followed by incubation in a freshly prepared nuclei staining buffer consisting of 250 μg/mL PI and 100 μg/mL RNase for 30 min at 37°C. Cell-cycle histograms were generated after analyzing the PI-stained cells by fluorescence-activated cell sorting (Beckman Coulter). Samples were analyzed using CXP software (Beckman Coulter), and proliferation indices [(S + G2/M)/(G0/G1 + S + G2/M)] × 100 were calculated.

Immunofluorescence staining

Cells were fixed with 3.5% paraformaldehyde, 0.1% Triton X-100, 5% BSA, and then treated with a 1:50 dilution of primary Ab against target protein. Each sample was then incubated for 30 min with a 1:100 dilution of FITC or Alexa Fluor 488-conjugated secondary Ab. Fluorescence images were visualized with a FluoView 300 fluorescence microscope (Olympus).

Duolink® fluorescence assay

Cx43/ZO-1 interaction was detected *in situ* using Duolink II secondary Abs and detection kits (Olink Bioscience; Cat#. 92001, 92005, and 92007) according to the manufacturer's instructions. Briefly, primary Abs against Cx43 (anti-mouse) and ZO-1 (anti-rabbit) were applied under standard conditions. Duolink secondary Abs against the primary Abs were then added. These secondary Abs were provided as conjugates to oligonucleotides that were ligated together in a closed circle by Duolink ligation solution if the Abs were in close proximity (< 40 nm). Finally, polymerase was added, which amplified any existing closed circles, and detection was achieved with complementary, fluorescently labeled oligonucleotides (green dot). PI staining (red) was used to verify cell morphology, and confocal images were acquired.

Cytosolic and total membrane fractionation

Cells were lysed in buffer A (137 mM NaCl, 8.1 mM Na_2HPO_4, 2.7 mM KCl, 1.5 mM KH_2PO_4, 2.5 mM EDTA, 1 mM dithiothreitol, 0.1 mM PMSF, and 10 μg/mL leupeptin [pH 7.5]). Resuspended cells were then mechanically lysed on ice by triturating with a 21.1-gauge needle. The lysates were first centrifuged at 1,000 *g* for 10 min at 4°C. Cytosolic and total particulate fractions were then prepared by centrifuging the supernatants at 100,000 *g* for 1 h at 4°C. The supernatants (cytosolic fraction) were then precipitated with 5 vol. of acetone, incubated for 5 min on ice, and centrifuged at 20,000 *g* for 20 min at 4°C. Pellets were resuspended in buffer A containing 1% (v/v) Triton X-100. The particulate fractions containing the membrane fraction were washed twice and resuspended in buffer A containing 1% (v/v) Triton X-100. Protein was quantified using the Bradford procedure [29].

Western blotting and immunoprecipitation

Proteins (20–40 μg) from cell homogenates were separated using 6%–15% sodium dodecyl sulfate polyacrylamide gel electrophoresis (SDS-PAGE) and transferred to polyvinylidene fluoride membranes. Each membrane was washed with Tris-buffered saline Tween-20 (TBST), consisting of 10 mM Tris-HCl (pH 7.6), 150 mM NaCl, and 0.05% Tween-20, blocked with 5% skim milk for 1 h, and incubated with the appropriate primary Abs at dilutions recommended by the supplier. Membranes were washed in TBST and probed with HRP-conjugated goat anti-rabbit or goat anti-mouse IgG secondary Ab. For immunoprecipitation, lysates were incubated with appropriate Abs and protein A-sepharose beads with gentle shaking overnight. Samples were washed thrice with lysis buffer and analyzed by SDS-PAGE. Bands were visualized with an enhanced chemiluminescence kit (Amersham Pharmacia Biotech) and quantified with TINA 2.0 software.

Small interfering ribonucleic acid transfection

Cells were grown until 75% of the plate surface was covered, after which they were transfected for 24 h with either a SMARTpool of small interfering ribonucleic acids (siRNAs) specific to ZO-1 or nontargeting siRNAs (as a negative control) (Dharmacon, Lafayette, CO) using Dharmafect transfection reagent (Dharmacon). After 24 h, the transfection mixtures were replaced with regular medium, and cells were maintained in normal culture conditions (DMEM supplemented with LIF and FBS) as they were before the experiments.

Affinity precipitation of cellular GTP-Rho

Ras homolog gene family, member A (RhoA) activation was determined using an affinity precipitation assay incorporating the glutathione-S-transferase (GST)-tagged fusion protein, corresponding to the Rhotekin Rho Binding Domain (RBD), which binds only the active GTP-bound form. Cells that had reached 70% confluence were incubated in the presence of laminin-111 for 30 min at 37°C before addition of lysis buffer (25 mM HEPES, [pH 7.5], 150 mM NaCl, 1% Igepal CA-630, 10 mM $MgCl_2$, 1 mM EDTA, 10% glycerol, 1 μg/mL aprotinin, 10 μg/mL leupeptin, and 1 mM Na_3VO_4) at 4°C. Whole cell lysates were incubated with agarose-conjugated GST-RBD 20 μg for 45 min at 4°C and then washed thrice with lysis buffer. In addition, whole cell lysates were incubated with GTPγS/GDP for 30 min at 30°C as positive/negative controls. Agarose beads were boiled in sample buffer to release active Rho. Sample proteins were resolved by 12% SDS-PAGE followed by immunoblotting with RhoA Ab.

Statistical analyses

All results are expressed as mean ± standard deviation (SD). All experiments were analyzed by analysis of variance. Several experiments were also evaluated by comparing the treatment means with the control using a Bonferroni–Dunn test. Statistical significance was defined at $P < 0.05$.

Results

Effect of ECM components on Cx43 functional changes

To identify Cx43 changes in mESCs in the presence of exogenous ECMs (laminin-111, fibronectin, and collagen I), we performed western blotting and SL/DT assays. Cx phosphorylation studies have focused on Cx43 due to its

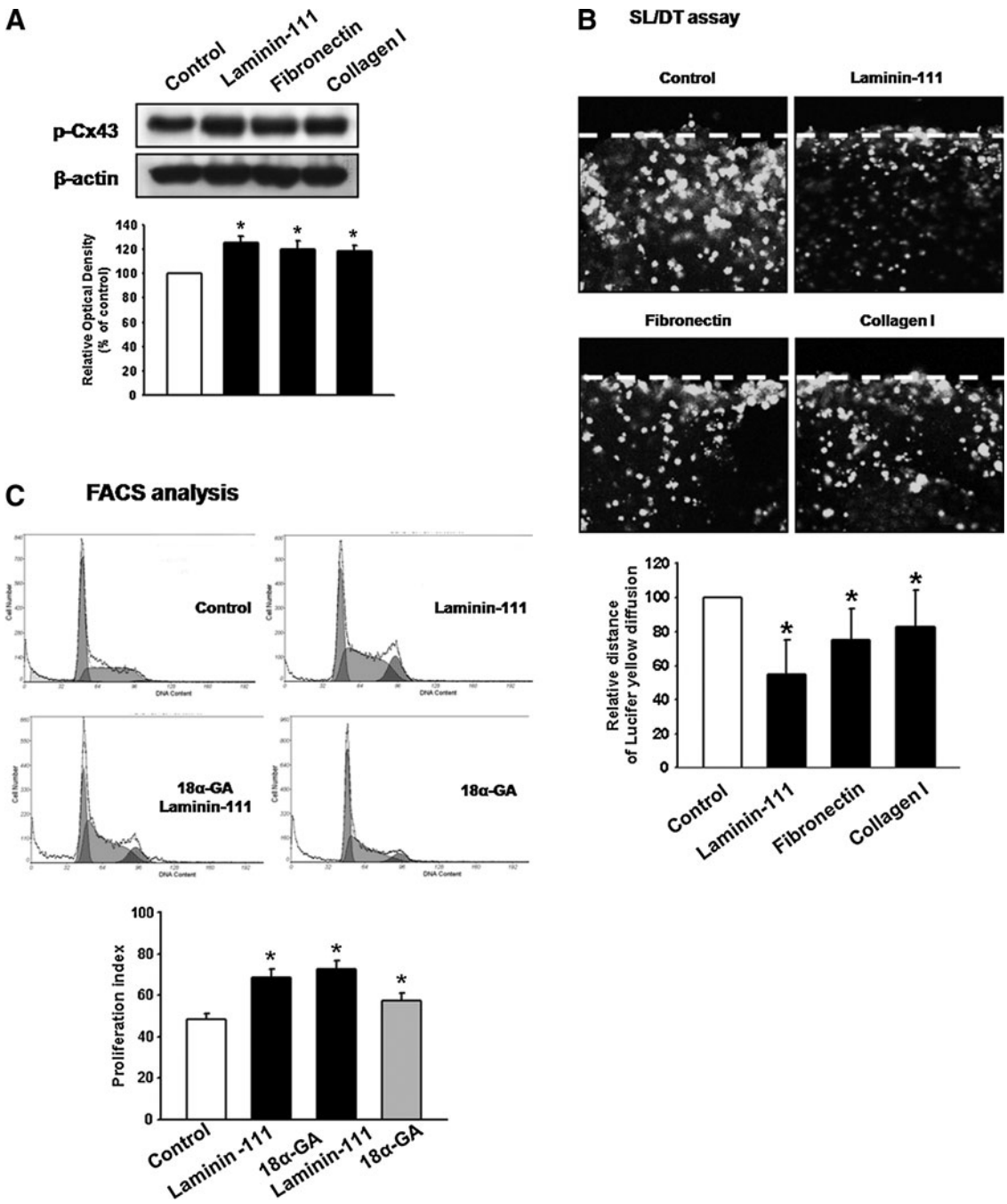

FIG. 1. Effect of extracellular matrix (ECM) component functional change on Cx43 and related mouse embryonic stem cell (mESC) proliferation **(A)** Cells were treated with laminin-111, fibronectin, or collagen I (10 μg/mL) for 30 min and the expression of p-Cx43 detected by western blot. The lower *panel* depicts the mean ± standard deviation (SD) of four independent experiments for each condition as determined from densitometry relative to β-actin. *$P < 0.05$ versus control. **(B)** Cells were treated with laminin-111, fibronectin, or collagen I for 30 min, and gap junctional intercellular communication (GJIC) analysis was carried out using a scrape loading/dye transfer (SL/DT) assay, as described in the Materials and Methods section. The lower *panel* depicts the mean ± SD of five independent experiments for each condition as determined from quantification of GJIC (the relative distance of Lucifer yellow diffusion compared with control). *$P < 0.05$ versus control. **(C)** Cells were treated with 18α-glycyrrhetinic acid (18α-GA, gap junction disruptor; 10 μg/mL) for 30 min before laminin-111 treatment for 24 h, harvested, and subjected to propidium iodide (PI) staining for cell-cycle analysis by flow cytometry. Gates were configured manually to determine the percentage of cells in S phase based on DNA content. Data are calculated using proliferation indices $[(S+G2/M)/(G0/G1+S+G2/M)] \times 100$ and reported as mean ± SD of four independent experiments, each conducted in triplicate. *$P < 0.05$ versus control.

importance within ESCs and directly regulated phosphorylation events. Therefore, we examined the effect of ECM components on phosphorylation of Cx43 and found that laminin-111, fibronectin, and collagen I (10 μg/mL) increased phosphorylation of Cx43 (Fig. 1A). Next, we examined GJIC in mESCs using the SL/DT assay with Ly. When cells treated with laminin-111, fibronectin, and collagen I were scraped and incubated in the presence of Ly, Ly remained at the site of the scrape, whereas extensive Ly diffusion through the colonies was observed in the control group. Mean ± SD (inch

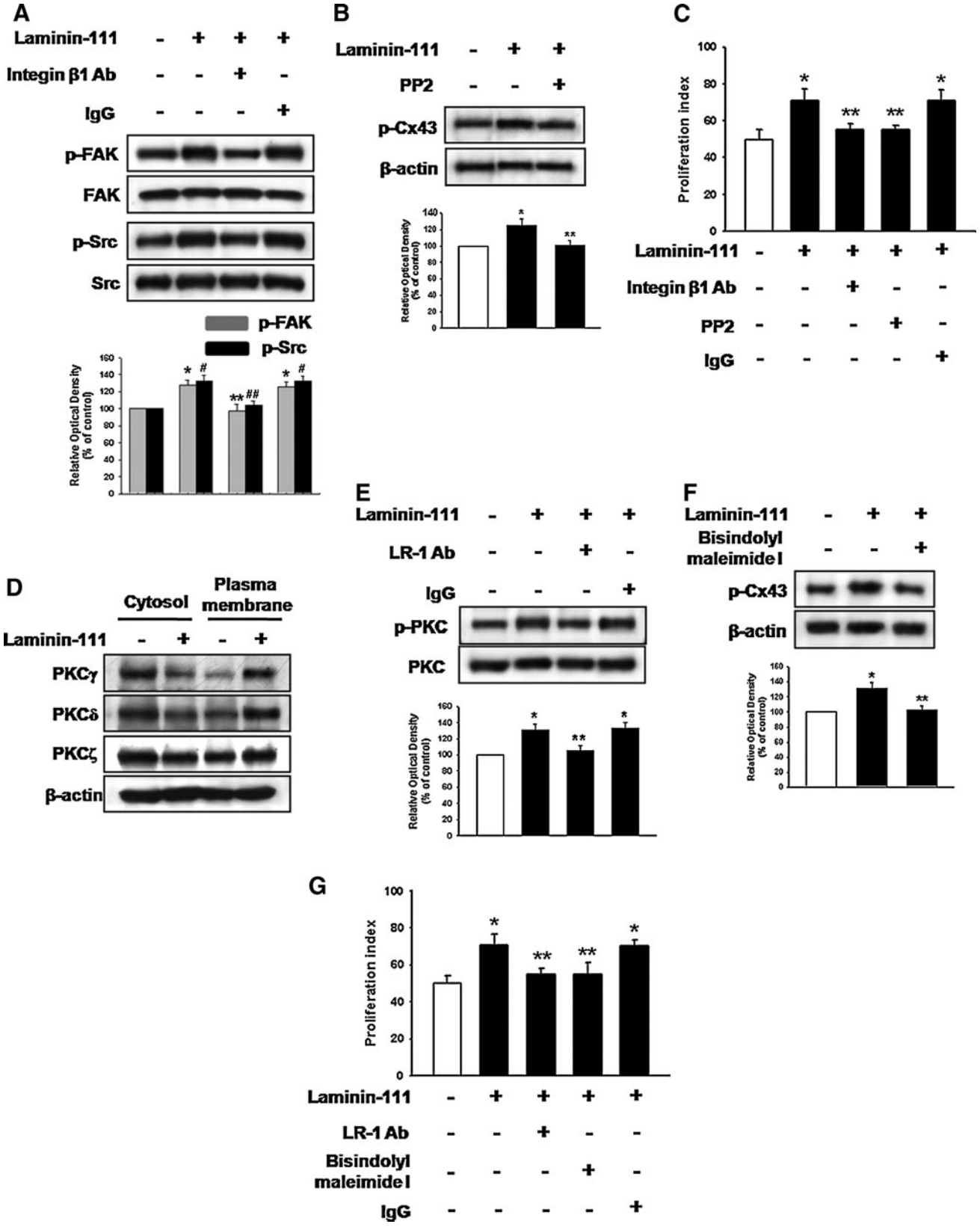

in photographs) of maximal distance of lateral spreading of Ly on mESCs treated with ECM components was significantly smaller than in control cells (Fig. 1B). Among ECM components, we found that laminin-111 affected functional regulation of Cx43 more intensive than fibronectin or collagen I; therefore, we chose laminin-111 as a ligand for further studies. Since the relationship between the proliferative capacity of mESCs and GJIC was ascertained, we treated cells with 18α-GA. A redistribution of Cx43 from cell-cell interfaces to cytoplasmic structures was reported after 18α-GA exposure [30]. In the present study, inactivation of Cx43 increased proliferation indices (Fig. 1C) (control: 48.50% ± 2.51%; laminin-111: 68.46% ± 4.01%; 18α-GA + laminin-111: 72.56% ± 3.96%; 18α-GA: 57.54% ± 3.54%). A possible mechanism responsible for this finding may involve interaction of Cx43 with other proteins and/or protein complexes that can regulate the cell cycle. Proteins such as ZO-1, εPKC, Src, or β-catenin, all of which have been implicated in the regulation of cell proliferation, are known to interact with Cx43 [31–34]. It is also theoretically possible that Cx43 may affect gene expression directly, acting as a transcription factor, or indirectly by interacting with transcription affecting protein(s) or complexes. Therefore, we examined related mechanisms of cell proliferation through reduction of GJIC induced by laminin-111.

Involvement of integrin β1/FAK/Src, LR-1/PKC, and RhoA on Cx43 phosphorylation

We examined the Cx43-related signal pathways affected by laminin-111. Laminin has several receptors, including integrins and LR-1. Functional blockage of integrin β1 inhibited laminin-111-induced phosphorylation of focal adhesion kinase (FAK) and Src (Fig. 2A) and inhibition of FAK/Src blocked phosphorylation of Cx43 (Fig. 2B). Moreover, inhibition of integrin β1 and FAK/Src decreased laminin-111-induced increase of cell proliferation (Fig. 2C). In addition, laminin-111 increased translocation of conventional, atypical, and novel PKC to the plasma membrane (Fig. 2D). Furthermore, LR-1-bound laminin-111 increased PKC phosphorylation (Fig. 2E), and laminin-111 increased Cx43 phosphorylation, which was blocked by bisindolylmaleimide I (PKC inhibitor) (Fig. 2F). Laminin-111 increased cell proliferation was decreased by functional blockage of LR-1 and inhibition of PKC kinase activity (Fig. 2G). Therefore, these results show that laminin-111-induced Cx43 phosphorylation and cell proliferation are mediated by integrin β1-mediated FAK/Src and LR-1-mediated PKC in parallel pathways. Rho GTPases are well-known cytoskeleton modulators in GJIC change; therefore, we examined the involvement of RhoA on Cx43 functional change. Laminin-111 increased activation of RhoA, which was blocked by FAK/Src inhibitor (PP2) and PKC inhibitor (bisindolylmaleimide I) (Fig. 3A), which suggests that integrin β1- or LR-1-dependent parallel pathways merge at RhoA. C3 is an ADP-ribosyltransferase from *Clostridium botulinum* that irreversibly inactivates RhoA by covalent modification. RhoA inhibitor C3 blocked Cx43 phosphorylation, whereas the Rho-associated kinase (ROCK) inhibitor Y27632 did not affect Cx43 phosphorylation (Fig. 3B). In addition, pretreatment with C3 reversed laminin-111 induced blockage of Ly diffusion (Fig. 3C), which suggests that RhoA might affect Cx43 independent of ROCK. Moreover, inhibition of RhoA decreased laminin-111-induced increase of cell proliferation (Fig. 3D).

Involvement of ZO-1 on laminin-induced junctional dissociation

Inhibition of RhoA decreased Cx43/ZO-1 protein interaction, whereas Cx43/ZO-2 interaction did not change (Fig. 4A). To confirm this result, subcellular localization of Cx43/ZO-1 interaction was visualized using a Duolink assay

FIG. 2. Involvement of integrin β1/FAK/Src and laminin receptor-1 (LR-1)/PKC on Cx43 phosphorylation **(A)** Cells were treated with integrin β1 neutralizing antibody (Ab, 1 μg/mL) or IgG (negative control; 1 μg/mL) for 30 min before laminin-111 treatment for 30 min, and expression of p-FAK or p-Src was detected by western blot. The lower *panel* depicts the mean ± SD of four independent experiments for each condition as determined from densitometry relative to FAK or Src. $^{*}P < 0.05$ versus control of p-FAK; $^{**}P < 0.05$ versus laminin-111 of p-FAK; $^{\#}P < 0.05$ versus control of p-Src; $^{\#\#}P < 0.05$ versus laminin-111 of p-Src. **(B)** Cells were treated with protein phosphatase 2 (PP2, FAK/Src inhibitor; 10^{-6} M) for 30 min before laminin-111 treatment for 30 min, and the expression of p-Cx43 was detected by western blot. The lower *panel* depicts the mean ± SD of three independent experiments for each condition as determined from densitometry relative to β-actin. $^{*}P < 0.05$ versus control; $^{**}P < 0.05$ versus laminin-111. **(C)** Cells were treated with integrin β1 neutralizing Ab, PP2, and IgG for 30 min before laminin-111 treatment for 24 h, harvested, and subjected to propidium iodide (PI) staining for cell-cycle analysis by flow cytometry. Gates were configured manually to determine the percentage of cells in the S phase based on DNA content. Data are calculated using proliferation indices $[(S+G2/M)/(G0/G1+S+G2/M)]\times 100$ and reported as mean ± SD of three independent experiments, each conducted in triplicate. $^{*}P < 0.05$ versus control;. $^{**}P < 0.05$ versus laminin-111. **(D)** Cells were treated with laminin-111 for 30 min, separated into cytosol and plasma membrane fractions, and the expression of PKCγ, PKCδ, or PKCζ protein detected by western blot. **(E)** Cells were treated with LR-1 neutralizing Ab (1 μg/mL) or IgG for 30 min before laminin-111 treatment for 30 min, and the expression of p-PKC was detected by western blot. The lower *panel* depicts the mean ± SD of four independent experiments for each condition as determined from densitometry relative to PKC. $^{*}P < 0.05$ versus control; $^{**}P < 0.05$ versus laminin-111. **(F)** Cells were treated with bisindolylmaleimide I (PKC inhibitor; 10^{-6} M) for 30 min before laminin-111 treatment for 30 min, and the expression of p-Cx43 was detected by western blot. The lower *panel* depicts the mean ± SD of three independent experiments for each condition as determined from densitometry relative to β-actin. $^{*}P < 0.05$ versus control; $^{**}P < 0.05$ versus laminin-111. **(G)** Cells were treated with LR-1 neutralizing Ab, bisindolylmaleimide I, or IgG for 30 min before laminin-111 treatment for 24 h, harvested, and subjected to propidium iodide (PI) staining for cell-cycle analysis by flow cytometry. Gates were configured manually to determine the percentage of cells in the S phase based on DNA content. Data are calculated using proliferation indices $[(S+G2/M)/(G0/G1+S+G2/M)]\times 100$ and reported as mean ± SD of three independent experiments, each conducted in triplicate. $^{*}P < 0.05$ versus control;. $^{**}P < 0.05$ versus laminin-111. FAK, focal adhesion kinase.

for Cx43/ZO-1 interaction. This assay works similarly to standard immunofluorescence detection, except that the secondary Abs are conjugated to oligonucleotides that comprise one-half of a closed circle that can be ligated together only when the Abs are in close proximity (<40 nm) [35]. This complex can then be detected by rolling circle amplification of the closed circle and addition of a complementary, fluorescently tagged oligonucleotide. Primary Abs against Cx43 and ZO-1 were used for Duolink detection of Cx43/ZO-1 interaction. Laminin-111 or calpeptin (Rho activator)-treated cells showed decreased proximity compared with controls or those pretreated with C3 (Fig. 4B). As we assumed ZO-1 to be related to GJIC, we transfected cells with ZO-1 siRNA and found that depletion of endogenous ZO-1 reduced GJIC intensively (Fig. 4C). ZO-1 siRNA transfection efficiency was examined using western blotting (Fig. 4D). Interestingly, laminin-111 also decreased ZO-1/tight junction proteins (claudin, occludin) or ZO-1/adherent junction proteins (E-cadherin, β-catenin) association (Fig. 4E). Moreover, inhibition of RhoA reversed the laminin-111-induced

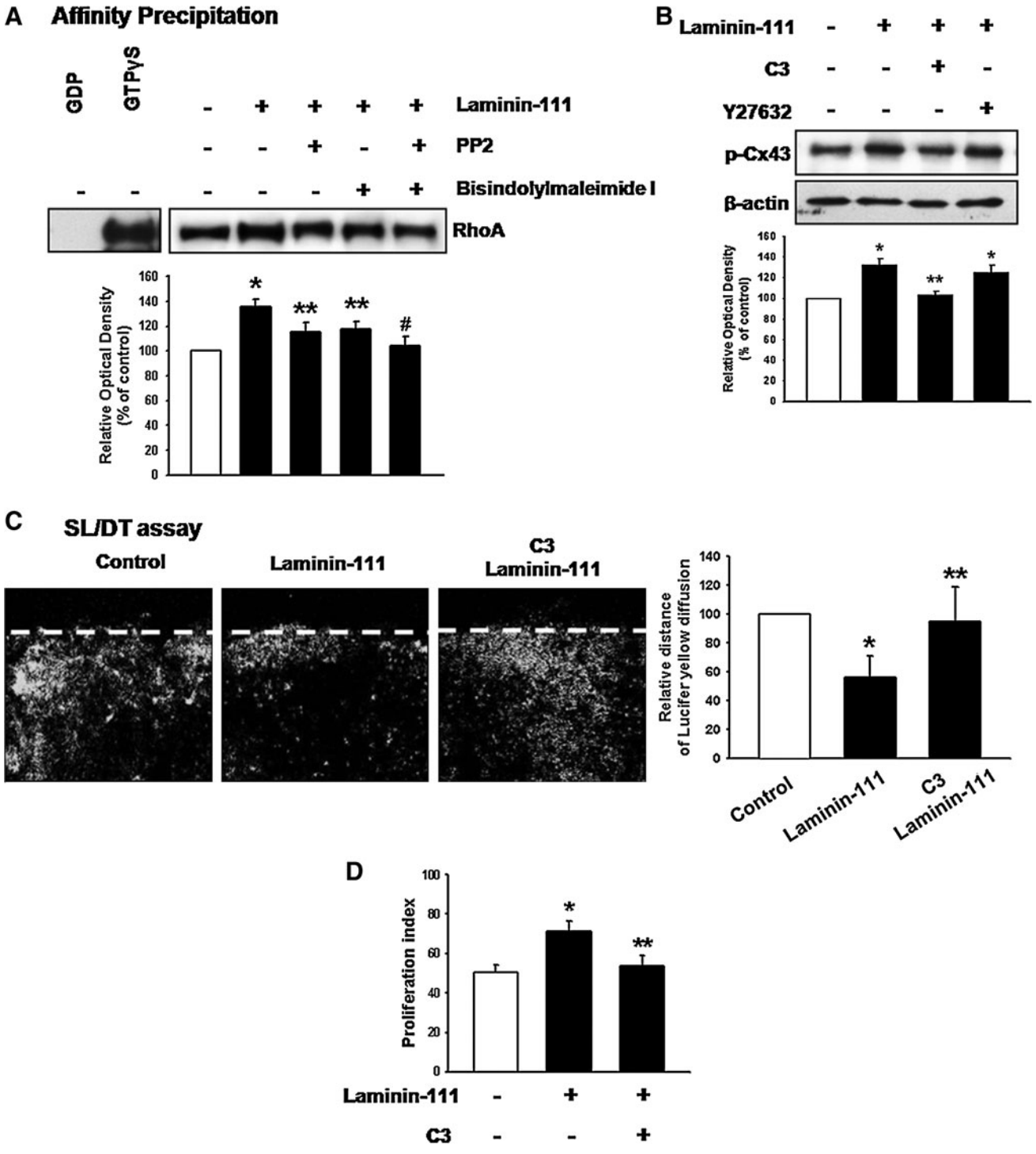

decrease of Cx43/F-actin and Cx43/drebrin complex (Fig. 5A). We confirmed this result using immunofluorescence staining. In control and C3 pretreatment cells, F-actin and Cx43 localization at the plasma membrane remained intact, whereas laminin-111 treated cells experienced decreased stabilization (Fig. 5B). Since a decrease of GJIC appeared to be involved in Cx43 degradation, cells were incubated with lysosomal protease inhibitor (chloroquine) or proteasome inhibitor (lactacystin), and then immunofluorescence was used to observe the localization of Cx43. Laminin-111-stimulated Cx43 labeling decreased at the plasma membrane as well as the intercellular junction, whereas cells that were pretreated with degradation inhibitors maintained Cx43 intercellularly (Fig. 5C, D).

Discussion

The present study indicates that laminin-111 stimulates mESC proliferation through reduction of GJIC via RhoA-induced Cx43 phosphorylation and Cx43/ZO-1/drebrin complex dissociation-induced degradation. To our knowledge, this is the first study describing the relationship between proliferation and reduction of GJIC through Cx43 macromolecule disruption. Integrins, receptors for ECM components, are not only mechanical receptors but also intracellular signal transducers. The laminin-receptor subgroup of integrins contains four heterodimers (α3β1, α6β1, α6β4, and α7β1), but α6β1 integrin is regarded as the specific receptor for laminin-111 in mESCs [36–38]. On the other hand, it could also bind to laminin-332 [39] and laminin-511/521 [40]. Indeed, laminin-511 has a higher effect on the cell proliferation and reduction of GJIC than laminin-111 in our experimental conditions (data not shown). This result indicates that LN-111 and LN-511 are preferred ligands with affinity toward α6β1 integrin in mouse ES cells. Based on previous reports, there was a striking difference in the effects of various laminin or integrin isoforms on ES cells [41–42]. This discrepancy could be due to a difference in laminin source and protocol for laminin purification even though same isotype of laminin as well as in vivo versus in vitro, animal species, cell types, experimental conditions, etc., used for study. FAK is activated by autophosphorylation in response to integrin ligation, which induces interaction with Src, leading to stable and increased activation of Src-FAK complex [43]. Our results showed that laminin-111 increased FAK and Src phosphorylation, which was blocked by integrin β1 neutralizing Ab. We found that c-Src is able to phosphorylate the Cx43 C-tail, and this phosphorylated residue behaved as a binding site for the c-Src SH2 domain. We also found that laminin-111-increased FAK/Src is related to phosphorylation of Cx43. In addition, LR-1 plays a role as a co-receptor of integrin and also has been shown to be an important step in the signal transduction pathway inducing tyrosine phosphorylation of signal transduction molecules [44–46]. In the present study, laminin-111 stimulated conventional, atypical, and novel PKC translocation from the cytosol to the plasma membrane, and functional blockage of LR-1 inhibited PKC phosphorylation. We also found that inhibition of PKC decreases Cx43 phosphorylation. A previous study reported that phosphorylation of purified human Cx43 resulted in only PKCε activation [47]. However, our results suggest that every type of PKC might be involved in Cx43 phosphorylation in mESCs. In the present study, inhibition of both FAK/Src and PKC blocked RhoA activation fully, which suggests that integrin β1/FAK/Src and LR-1/PKC parallel pathways merge at RhoA. Rho GTPase is known as a major regulator of cellular junctions [48–49]. In the present study, both a decrease of Cx43 phosphorylation and an induction of intercellular coupling were observed after C3 (RhoA inhibitor) exposure, suggesting that RhoA modulates junctional channel functions. However, inhibition of ROCK did not block Cx43 phosphorylation. This result indicates that RhoA does not influence junctional permeability through its downstream effector ROCK, consistent with the results of a previous study [50]. Based on this information, using mESCs, we demonstrated a correlation between laminin-111 and Cx dependence on the coordinated action of at least two signaling systems, direct integrin-dependent FAK/Src signaling, and the LR-dependent PKC pathways that merge at RhoA.

There is a growing understanding that an array of proteins interact with Cx, potentially mediating linkage of GJs to other junction types, signal transduction molecules, and the cytoskeleton. One Cx-interacting molecule that has received

FIG. 3. Involvement of Ras homolog gene family, member A (RhoA) on Cx43 phosphorylation. **(A)** Cells were treated with PP2 or/and bisindolylmaleimide I for 30 min before laminin-111 treatment and then loaded with GDP (negative control; lane 1) or GTPγS (positive control; lane 2) before affinity precipitation in the presence of 10 μg of glutathione-S-transferase- Rho Binding Domain on glutathione-sepharose beads. After each binding reaction at 4°C, the proteins bound to the beads were separated by 15% sodium dodecyl sulfate polyacrylamide gel electrophoresis (SDS-PAGE) and examined for GTP-bound RhoA. The lower *panel* depicts the mean ± SD of three independent experiments for each condition. $^{*}P < 0.05$ versus control; $^{**}P < 0.05$ versus laminin-111; $^{\#}P < 0.05$ versus PP2 with laminin-111 or bisindolylmaleimide I with laminin-111. **(B)** Cells were treated with C3 (RhoA inhibitor; 1 μg/mL) or Y27632 (ROCK inhibitor; 10^{-6} M) for 30 min before laminin-111 treatment for 30 min, and the expression of p-Cx43 was detected by western blot. The lower *panel* depicts the mean ± SD of three independent experiments for each condition as determined from densitometry relative to β-actin. $^{*}P < 0.05$ versus control; $^{**}P < 0.05$ versus laminin-111. **(C)** Cells were treated with C3 for 30 min before laminin-111 treatment for 30 min, and GJIC analysis was carried out using a scrape loading/dye transfer (SL/DT) assay, as described in the Materials and Methods section. The lower *panel* depicts the mean ± SD of four independent experiments for each condition as determined from quantification of GJIC (the relative distance of Lucifer yellow diffusion compared with control). $^{*}P < 0.05$ versus control; $^{**}P < 0.05$ versus laminin-111. **(D)** Cells were treated with C3 for 30 min before laminin-111 treatment for 24 h, harvested, and subjected to propidium iodide (PI) staining for cell-cycle analysis by flow cytometry. Gates were configured manually to determine the percentage of cells in the S phase based on DNA content. Data are calculated using proliferation indices $[(S+G2/M)/(G0/G1+S+G2/M)] \times 100$ and reported as mean ± SD of three independent experiments, each conducted in triplicate. $^{*}P < 0.05$ versus control;. $^{**}P < 0.05$ versus laminin-111. ROCK , Rho-associated kinase.

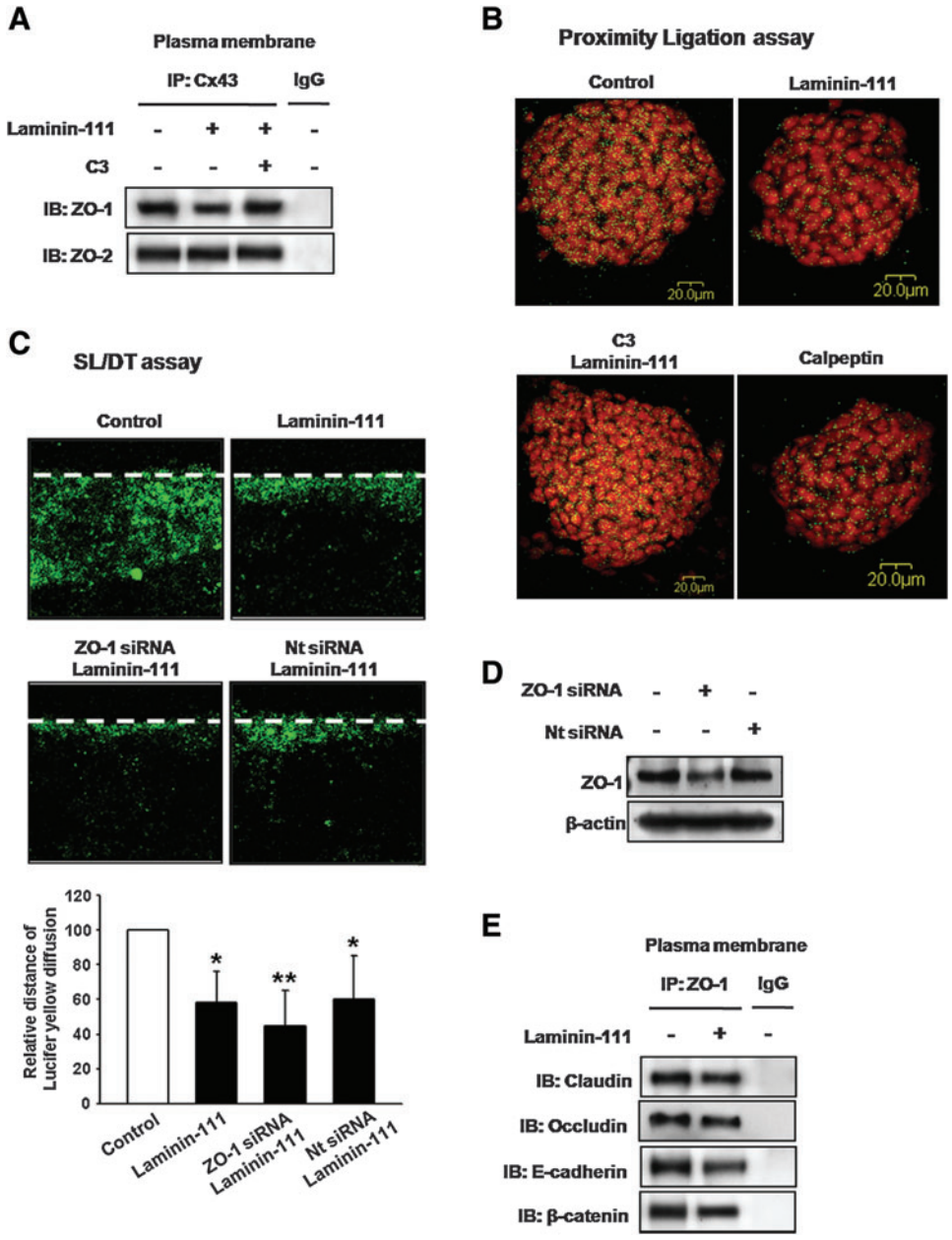

FIG. 4. Involvement of Cx43/ZO-1 complex on GJIC stability **(A)** Cells were treated with C3 for 30 min before laminin-111 treatment for 30 min, and then, plasma membrane fraction was isolated. Plasma membrane protein lysates were immunoprecipitated with an anti-Cx43 Ab and blotted with Abs directed against ZO-1 or ZO-2. The example shown is representative of five independent experiments. **(B)** Cells were treated with C3 for 30 min before laminin-111 treatment for 30 min or calpeptin (Rho activator; 0.5 unit/mL) for 30 min. Duolink® fluorescence (Cx43/ZO-1 interaction; *green* dot) and PI (*red*) were assessed. The example shown is representative of five independent experiments. **(C)** Cells were transfected with ZO-1 siRNA (20 μM) or Nt siRNA (negative control; 20 μM) for 24 h before laminin-111 treatment for 30 min, and GJIC analysis was carried out using an SL/DT assay, as described in the Materials and Methods section. The lower *panel* depicts the mean ± SD of four independent experiments for each condition as determined from quantification of GJIC (the relative distance of Lucifer yellow diffusion compared with control). $^{*}P < 0.05$ versus control; $^{**}P < 0.05$ versus laminin-111. **(D)** Cells were transfected with ZO-1 siRNA or Nt siRNA for 24 h, and the expression of ZO-1 was detected by western blot. The example shown is representative of two independent experiments. **(E)** Cells were treated with laminin-111 for 30 min, and then, the plasma membrane fraction was isolated. Plasma membrane protein lysates were immunoprecipitated with an anti-ZO-1 Ab and blotted with Abs directed against claudin, occludin, E-cadherin, or β-catenin. The example shown is representative of three independent experiments. Color images available online at www.liebertonline.com/scd

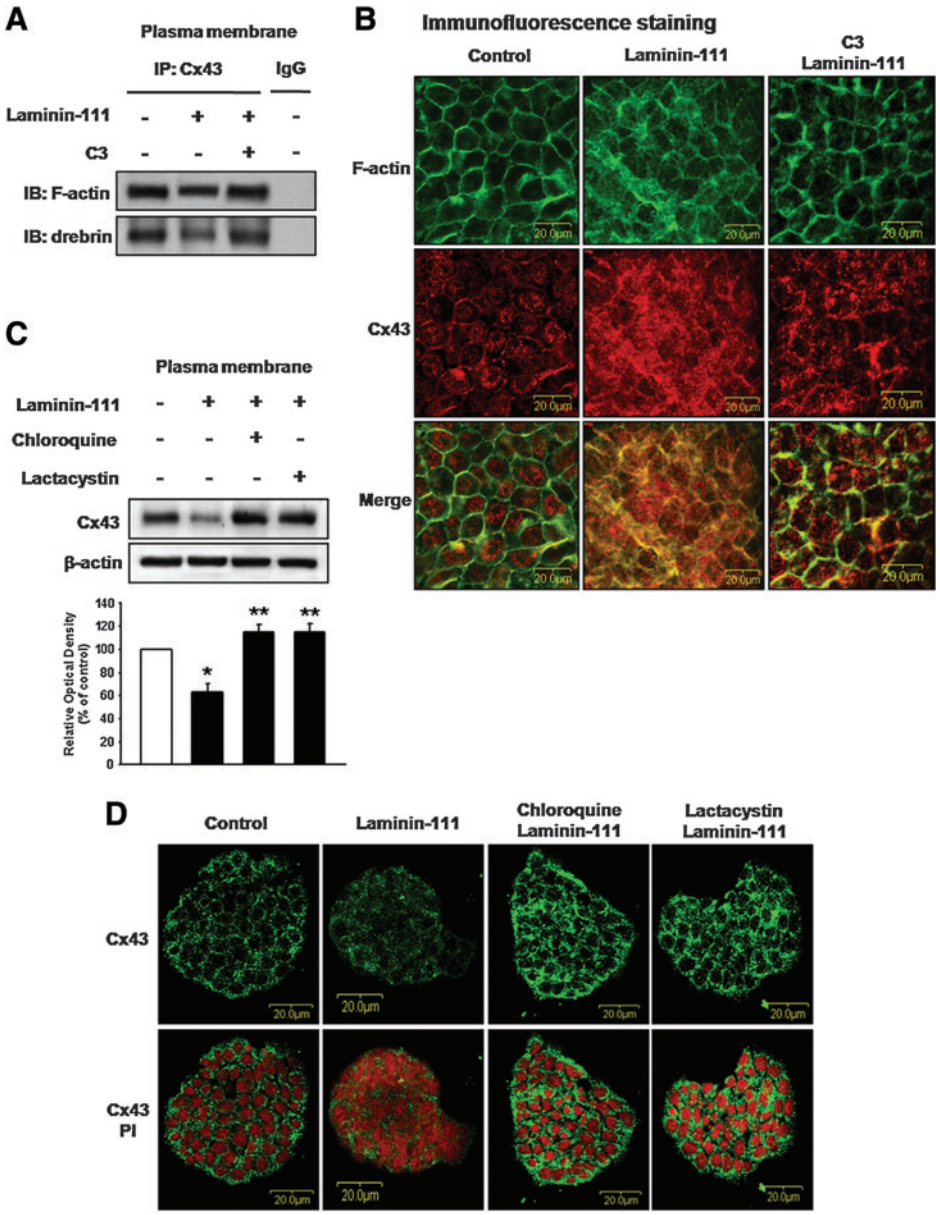

FIG. 5. Involvement of Cx43/cytoskeleton complex on GJIC degradation. **(A)** Cells were treated with C3 for 30 min before laminin-111 treatment for 30 min, separated into plasma membrane, and then, the lysates were immunoprecipitated with an anti-Cx43 Ab and blotted with Abs directed against F-actin or drebrin. The example shown is representative of four independent experiments. **(B)** Cells were treated with C3 for 30 min before laminin-111 treatment for 30 min, and immunofluorescence staining with F-actin (*green*) or Cx43 (*red*) was assessed. Cells were treated with chloroquine (lysosomal protease inhibitor; 10^{-4} M), or lactacystin (proteasome inhibitor; 10^{-5} M) for 30 min before laminin-111 treatment for 30 min, and then, the plasma membrane fraction was isolated. The expression of Cx43 at plasma membrane detected by western blot **(C)** and immunofluorescence staining with Cx43 (*green*) and PI (*red*) were assessed **(D)**. The lower *panel* depicts the mean ± SD of three independent experiments for each condition. $^{*}P < 0.05$ versus control; $^{**}P < 0.05$ versus laminin-111. Color images available online at www.liebertonline.com/scd

particular attention is ZO-1. Originally identified as a component of tight junctions, ZO-1, ZO-2, and ZO-3 are members of the membrane-associated guanylate kinase family of proteins [51–52]. ZO-1, in particular, has been shown to interact with the carboxy terminus of Cx43, and Cx43/ZO-1 interaction is involved in GJ regulation [53]. ZO-2 was also reported to bind to the Cx43 tail in vitro, independent of ZO-1 [54]. The functional significance of ZO-1 or ZO-2 interaction with Cx43 is not as yet well defined; however, a few studies reported that these proteins are not functionally redundant [55]. In the present study, ZO-1 and ZO-2 were expressed in mESCs, and laminin-111 dissociated the Cx43/ZO-1 association, while Cx43/ZO-2 was not affected, which suggests that ZO-1 is involved in Cx43 regulation. Duolink assay data provided strong evidence into the Cx43/ZO-1 interaction. Under control or C3 (RhoA inhibitor) pretreated cells, it was found that the Cx43/ZO-1 interaction (green dot) occurred throughout cells, especially at cell-cell borders. However, decreased Duolink fluorescence was observed in laminin-111 or calpeptin (Rho activator)-treated cells. This result suggests a relationship between Rho GTPases and Cx43/ZO-1 complex. Derangeon et al. [56] reported that RhoA inhibition caused an increase of the Cx43/ZO-1 association modulating the phosphorylation/dephosphorylation cycle of Cx43. Divergent roles have been proposed for Cx43/ZO-1 interaction, including the control of GJ formation and localization of GJ plaques, as well as internalization of Cx43 and its targeting for endocytosis. In osteoblastic cells, disruption of the Cx43/ZO-1 interaction with a Cx-binding fusion protein derived from ZO-1 disrupted GJ formation and function, whereas overexpression of ZO-1 enhanced both junctional plaques and GJIC [57]. The down-regulation of ZO-1 in N/N1003A lens epithelial cells also resulted in loss-of-dye transfer activity without altering the total amount of Cx43 protein in cells [58]. In mESCs, we found that depletion of ZO-1 blocked GJIC. The present results provide further insight into the gating and regulation of junctional channels, confirming the important role of ZO-1 in the

function of Cx43 GJs, and identifying a new downstream target for the small G-protein RhoA. These interactions with other proteins are required for connexon assembly, transport via microtubules from Golgi apparatus to the plasma membrane GJ plaque, and degradation.

Recent studies revealed that Cxs can interact with a large number of additional partners and drebrin has been focused on more recently. Actin might be linked to GJs by drebrin and thereby stabilize Cx43 at the plasma membrane, possibly by preventing interaction with degradation machinery or by forming a highly structured complex between Cx43 and the cytoskeleton [59]. A role for ZO-1 in linking the actin cytoskeleton and GJs is supported by coprecipitation of both actin and ZO-1 with Cx43. In the present study, laminin-111 dissociated Cx43/F-actin and Cx43/drebrin protein complexes. Therefore, we hypothesized that disruption of Cx43/cytoskeleton association occurs along with Cx43/ZO-1 complex dissociation, and this series of events leads to destabilization of GJIC or other cell junctions. Decreased GJIC is closely related to cellular processes such as trafficking, assembly/disassembly, gating of GJ channels, and altered susceptibility to degradation [60–61]. Internalized GJs require proteasomal activity [62] and are degraded in lysosomes [63]. Western blotting or Immunofluorescence staining showed laminin changed Cx43 distribution from the plasma membrane to within whole cells, which was blocked by lysosomal protease inhibitor (chloroquine) or proteasome inhibitor (lactacystin), suggesting that laminin-111 stimulates Cx43 degradation. Taken together, our data reveal that laminin-111 leads to severe disruption of cell-cell communication by interfering with GJ plaques after the rapid internalization of these structures. It is possible that this step is associated with cytoskeletal movements implicated in the endocytic process, the nature of which remains to be identified. These data may improve understanding of the role of laminin-111 in regulating the expression of Cx43, which is crucial for controlling ESC growth, dysregulation of which may materially contribute to the pluripotency of ESCs. In conclusion, we determined that laminin-111 stimulated mESC proliferation through a reduction of GJIC, via integrins β1/FAK/Src and LR-1/PKC, which merge at RhoA-mediated Cx43 phosphorylation, and dissociation of Cx43/ZO-1/drebrin complex-mediated Cx43 endocytosis.

Acknowledgment

This research was supported by a National Research Foundation grant funded by the Korean government (MEST) (No. 2009-0081395; 2010-0020268) and the Biotherapy Human Resources Center (Brain Korea 21) project.

Author Disclosure Statement

No competing financial interests exist.

References

1. Koide T and Y Ito. (2000). Juxtacrine and matricrine—the other ways of growth factor actions. Seikagaku 72:1259–1263.
2. Miyamoto S, M Nakamura, K Yano, G Ishii, T Hasebe, Y Endoh, T Sangai, H Maeda, Z Shi-Chuang, T Chiba and A Ochiai. (2007). Matrix metalloproteinase-7 triggers the matricrine action of insulin-like growth factor-II via proteinase activity on insulin-like growth factor binding protein 2 in the extracellular matrix. Cancer Sci 98:685–691.
3. Aszódi A, KR Legate, I Nakchbandi and R Fässler. (2006). What mouse mutants teach us about extracellular matrix function. Annu Rev Cell Dev Biol 22:591–621.
4. Yurchenco PD, Y Quan, H Colognato, T Mathus, D Harrison, Y Yamada and JJ O'Rear. (1997). The α chain of laminin-1 is independently secreted and drives secretion of its β- and γ-chain partners. Proc Natl Acad Sci U S A 94:10189–10194.
5. Yurchenco P. (2003). Laminin 2 and methods for its use. United States patent #6,632,790.
6. Boutaud A. (2004). Recombinant laminin 5. United States Patent #6,703,363.
7. Kortesmaa J, P Yurchenco and K Tryggvason. (2000). Recombinant laminin-8 (α4β1γ1). Production, purification, and interactions with integrins. J Biol Chem 275:14853–14859.
8. Doi M, J Thyboll, J Kortesmaa, K Jansson, A Iivanainen, M Parvardeh, R Timpl, U Hedin, J Swedenborg and K Tryggvason. (2002). Recombinant human laminin-10 (α5β1γ1). Production, purification, and migration-promoting activity on vascular endothelial cells. J Biol Chem 277:12741–12748.
9. Imbeault S, LG Gauvin, HD Toeg, A Pettit, CD Sorbara, L Migahed, R DesRoches, AS Menzies, K Nishii, DL Paul, AM Simon and SA Bennett. (2009). The extracellular matrix controls gap junction protein expression and function in postnatal hippocampal neural progenitor cells. BMC Neurosci 10:13.
10. Lampe PD, BP Nguyen, S Gil, M Usui, J Olerud, Y Takada and WG Carter. (1998). Cellular interaction of integrin α3β1 with laminin 5 promotes gap junctional communication. J Cell Biol 143:1735–1747.
11. Guo Y, C Martinez-Williams, CE Yellowley, HJ Donahue and DE Rannels. (2001). Connexin expression by alveolar epithelial cells is regulated by extracellular matrix. Am J Physiol Lung Cell Mol Physiol 280:L191–L202.
12. Isakson BE, CE Olsen and S Boitano. (2006). Laminin-332 alters connexin profile, dye coupling and intercellular Ca^{2+} waves in ciliated tracheal epithelial cells. Respir Res 7:105.
13. Goodenough DA, JA Goliger and DL Paul. (1996). Connexins, connexons, and intercellular communication. Annu Rev Biochem 65:475–502.
14. Guthrie SC and NB Gilula. (1989). Gap junctional communication and development. Trends Neurosci 12:12–16.
15. Loewenstein WR. (1979). Junctional intercellular communication and the control of growth. Biochim Biophys Acta 560:1–65.
16. Mehta PP, JS Bertram and WR Loewenstein. (1986). Growth inhibition of transformed cells correlates with their junctional communication with normal cells. Cell 44: 187–196.
17. Solan JL and PD Lampe. (2005). Connexin phosphorylation as a regulatory event linked to gap junction channel assembly. Biochim Biophys Acta 1711:154–163.
18. Moreno AP. (2005). Connexin phosphorylation as a regulatory event linked to channel gating. Biochim Biophys Acta 1711:164–171.
19. Chambers I. (2004). The molecular basis of pluripotency in mouse embryonic stem cells. Cloning Stem Cells 6:386–391.
20. O'Shea KS. (2004). Self-renewal vs. differentiation of mouse embryonic stem cells. Biol Reprod 71:1755–1765.
21. Trosko JE, CC Chang, BL Upham and MH Tai. (2004). Ignored hallmarks of carcinogenesis: stem cells and cell-cell communication. Ann N Y Acad Sci 1028:192–201.

22. Wong RC, A Pébay, LT Nguyen, KL Koh and MF Pera. (2004). Presence of functional gap junctions in human embryonic stem cells. Stem Cells 22:883–889.
23. Carpenter MK, ES Rosler, GJ Fisk, R Brandenberger, X Ares, T Miura, M Lucero and MS Rao. (2004). Properties of four human embryonic stem cell lines maintained in a feeder-free culture system. Dev Dyn 229:243–258.
24. Oyamada M, H Kimura, Y Oyamada, A Miyamoto, H Ohshika and M Mori. (1994). The expression, phosphorylation, and localization of connexin 43 and gap-junctional intercellular communication during the establishment of a synchronized contraction of cultured neonatal rat cardiac myocytes. Exp Cell Res 212:351–358.
25. Kim MO, YJ Lee and HJ Han. (2010). Involvement of Cx43 phosphorylation in 5′-N-ethylcarboxamide-induced migration and proliferation of mouse embryonic stem cells. J Cell Physiol 224:187–194.
26. Park JH, MY Lee, JS Heo and HJ Han. (2008). A potential role of connexin 43 in epidermal growth factor-induced proliferation of mouse embryonic stem cells: involvement of Ca^{2+}/PKC, p44/42 and p38 MAPKs pathways. Cell Prolif 41:786–802.
27. El-Fouly MH, JE Trosko and CC Chang. (1987). Scrape-loading and dye transfer: a rapid and simple technique to study gap junctional intercellular communication. Exp Cell Res 168:422–430.
28. Zhang Y, Y Kakinuma, M Ando, RG Katare, F Yamasaki, T Suqiura and T Sato. (2006). Acetylcholine inhibits the hypoxia-induced reduction of connexin43 protein in rat cardiomyocytes. J Pharmacol Sci 101:214–222.
29. Bradford MM. (1976). A rapid and sensitive method for the quantitation of microgram quantities of protein utilizing the principle of protein-dye binding. Anal Biochem 72: 248–254.
30. Talhouk RS, R Mroue, M Mokalled, L Abi-Mosleh, R Nehme, A Ismail, A Khalil, M Zaatari and ME El-Sabban. (2008). Heterocellular interaction enhances recruitment of α and β-catenins and ZO-2 into functional gap-junction complexes and induces gap junction-dependant differentiation of mammary epithelial cells. Exp Cell Res 314:3275–3291.
31. Ai Z, A Fischer, DC Spray, AM Brown and GI Fishman. (2000). Wnt-1 regulation of connexin43 in cardiac myocytes. J Clin Invest 105:161–171.
32. Doble BW, P Ping and E Kardami. (2000). The epsilon subtype of protein kinase C is required for cardiomyocyte connexin-43 phosphorylation. Circ Res 86:293–301.
33. Giepmans BN, I Verlaan and WH Moolenaar. (2001). Connexin-43 interactions with ZO-1 and α- and β-tubulin. Cell Commun Adhes 8:219–223.
34. Lin R, BJ Warn-Cramer, WE Kurata and AF Lau. (2001). v-Src-mediated phosphorylation of connexin43 on tyrosine disrupts gap junctional communication in mammalian cells. Cell Commun Adhes 8:265–269.
35. Jarvius M, J Paulsson, I Weibrecht, KJ Leuchowius, AC Andersson, C Wählby, M Gullberg, J Botling, T Sjöblom, et al. (2007). *In situ* detection of phosphorylated platelet-derived growth factor receptor β using a generalized proximity ligation method. Mol Cell Proteomics 6:1500–1509.
36. Suh HN and HJ Han. (2010). Laminin regulates mouse embryonic stem cell migration: involvement of Epac1/Rap1 and Rac1/cdc42. Am J Physiol Cell Physiol 298:C1159–C1169.
37. Aumailley M, R Timpl and A Sonnenberg. (1990). Antibody to integrin alpha6 subuint specifically inhibits cell-binding to laminin fragment 8. Exp Cell Res 188:55–60.
38. Sonnenberg A, CC Linders, PP Modderman, CC Damksy, M Aumailley and R Timple. (1990). Integrin recognition of different cell-bindign fragments of laminin (P1, E3, E8) and evidence ath α6β1 but not α6β4 functions as a major receptor for fragment E8. J Cell Biol 110: 2145–2155.
39. Delwel GG, AA de Melker, F Hogervoorst, LL Jaspars, DD Fles, I Kuikman, A Lindblom, M Paulsson, R Timple and A Sonneber. (1994). Distinct and overlapping ligand specificites of the α3Aβ1 and α6Aβ1 integrins: recognition of laminin isoforms. Mol Biol Cell 5:203–215.
40. Kikkawa Y, N Sanzen, H Fujiwara, A Sonnenber and K Sekiguchi. (2000). Integrin binding sepecificity of laminin-10/11 are recognized by α3β1, α6β1 and α6β4 integrins. J Cell Sci 113:869–876.
41. Nishiuchi R, O Murayama, H Fujiwara, J Gu, T Kawakami, S Aimoto, Y Wada and K Sekiguchi. (2003). Characterization of the ligand-binding specificities of integrin α3β1 and α6β1 using a panel of purified laminin isoforms containing distinct αβchains. J Biochem. 134:497–504.
42. Domogatskaya A, S Rodin, A Boutaud and K Tryggvason. (2008). Lamin-511 but not -332, -111, or -411 enables mouse embryonic stem cell self-renewal *in vitro*. Stem Cells 26: 2800–2809.
43. Wei Y, X Yang, Q Liu, JA Wilkins and HA Chapman. (1999). A role for caveolin and the urokinase receptor in integrin-mediated adhesion and signaling. J Cell Biol 144:1285–1294.
44. Gloe T, S Riedmayr, HY Sohn and U Pohl. (1999). The 67-kDa laminin-binding protein is involved in shear stress-dependent endothelial nitric-oxide synthase expression. J Biol Chem 274:15996–16002.
45. Bushkin-Harav I and UZ Littauer. (1998). Involvement of the YIGSR sequence of laminin in protein tyrosine phosphorylation. FEBS Lett 424:243–247.
46. Givant-Horwitz V, B Davidson and R Reich. (2004). Laminin-induced signaling in tumor cells: the role of the M(r) 67,000 laminin receptor. Cancer Res 64:3572–3579.
47. Hervé JC and D Sarrouilhe. (2006). Protein phosphatase modulation of the intercellular junctional communication: importance in cardiac myocytes. Prog Biophys Mol Biol 90:225–248.
48. Hall A. (1998). Rho GTPases and the actin cytoskeleton. Science 279:509–514.
49. Etienne-Manneville S and A Hall. (2002). Rho GTPases in cell biology. Nature 420:629–635.
50. Verrecchia F and J Hervé. (1997). Reversible inhibition of gap junctional communication by tamoxifen in cultured cardiac myocytes. Pflugers Arch 434:113–116.
51. Gumbiner B, T Lowenkopf and D Apatira. (1991). Identification of a 160-kDa polypeptide that binds to the tight junction protein ZO-1. Proc Natl Acad Sci U S A 88:3460–3464.
52. Jesaitis LA and DA Goodenough. (1994). Molecular characterization and tissue distribution of ZO-2, a tight junction protein homologous to ZO-1 and the Drosophila discs-large tumor suppressor protein. J Cell Biol 124:949–961.
53. Giepmans BN and WH Moolenaar. (1998). The gap junction protein connexin43 interacts with the second PDZ domain of the zona occludens-1 protein. Curr Biol 8:931–934.
54. Singh D and PD Lampe. (2003). Identification of connexin-43 interacting proteins. Cell Commun Adhes 10:215–220.
55. Umeda K, T Matsui, M Nakayama, K Furuse, H Sasaki, M Furuse and S Tsukita. (2004). Establishment and characterization of cultured epithelial cells lacking expression of ZO-1. J Biol Chem 279:44785–44794.

56. Derangeon M, N Bourmeyster, I Plaisance, C Pinet-Charvet, Q Chen, F Duthe, MR Popoff, D Sarrouilhe and JC Hervé. (2008). RhoA GTPase and F-actin dynamically regulate the permeability of Cx43-made channels in rat cardiac myocytes. J Biol Chem 283:30754–30765.
57. Laing JG, BC Chou and TH Steinberg. (2005). ZO-1 alters the plasma membrane localization and function of Cx43 in osteoblastic cells. J Cell Sci 118:2167–2176.
58. Akoyev V and DJ Takemoto. (2007). ZO-1 is required for protein kinase C γ-driven disassembly of connexin 43. Cell Signal 19:958–967.
59. Butkevich E, S Hülsmann, D Wenzel, T Shirao, R Duden and I Majoul. (2004). Drebrin is a novel connexin-43 binding partner that links gap junctions to the submembrane cytoskeleton. Curr Biol 14:650–658.
60. Lampe PD and AF Lau. (2000). Regulation of gap junctions by phosphorylation of connexins. Arch Biochem Biophys 384:205–215.
61. Ruch RJ, JE Trosko and BV Madhukar. (2001). Inhibition of connexin43 gap junctional intercellular communication by TPA requires ERK activation. J Cell Biochem 83:163–169.
62. Leithe E and E Rivedal. (2004). Ubiquitination and down-regulation of gap junction protein connexin-43 in response to 12-O-tetradecanoylphorbol 13-acetate treatment. J Biol Chem 279:50089–50096.
63. Lan Z, WE Kurata, KD Martyn, C Jin and AF Lau. (2005). Novel rab GAP-like protein, CIP85, interacts with connexin43 and induces its degradation. Biochemistry 44:2385–2396.

Address correspondence to:
Prof. Ho Jae Han
Department of Veterinary Physiology
College of Veterinary Medicine
Seoul National University
Seoul, 151-741
South Korea

E-mail: hjhan@snu.ac.kr

Received for publication September 6, 2011
Accepted after revision December 7, 2011
Prepublished on Liebert Instant Online December 7, 2011